metals

MDPI

Review

Wear Performance of Metal Materials Fabricated by Powder Bed Fusion: A Literature Review

Hongling Qin [1], Runzhou Xu [1], Pixiang Lan [2], Jian Wang [3] and Wenlong Lu [3,*]

[1] Hubei Key Laboratory of Hydroelectric Machinery Design & Maintenance, China Three Gorges University, Yichang 443000, China; qhl@ctgu.edu.cn (H.Q.); xrz19950104@outlook.com (R.X.)
[2] ATSP Innovations, Champaign, IL 61820, USA; lanpixiang@gmail.com
[3] The State Key Laboratory of Digital Manufacturing Equipment and Technology, School of Mechanical Science and Engineering, Huazhong University of Science and Technology, Wuhan 430074, China; jianwang@hust.edu.cn
* Correspondence: hustwenlong@hust.edu.cn

Received: 26 November 2019; Accepted: 17 February 2020; Published: 26 February 2020

check for updates

Abstract: Powder Bed Fusion (PBF) is an additive manufacturing technology used to produce metal-based materials. PBF materials have a unique microstructure as a result from repeated and sharp heating/cooling cycles. Many researches have been carried out on relations between processing parameters of the PBF technology, obtained microstructures and mechanical properties. However, there are few studies on the tribological properties of PBF materials at various contact conditions. This article describes previous and recent studies related to the friction performance. This is a critical aspect if PBF materials are applied to friction pair components. This paper discusses wear rates and wear mechanisms of PBF materials under dry friction, boundary lubrication and micro-motion conditions. PBF materials have higher hardness due to fine grains. PBF materials have a higher wear resistance than traditional materials due to their solid solution strengthening. In addition, hard particles on the surface of PBF components can effectively reduce wear. The reasonable combination of process parameters can effectively improve the density of parts and thus further improve the wear resistance. This review paper summarized the wear behavior of PBF materials, the wear mechanism of metal materials from dry friction to different lubrication conditions, and the wear behavior under fretting wear. This will help to control the processing parameters and material powder composition of parts, so as to achieve the required material properties of parts and further improve the wear performance.

Keywords: additive manufacturing; powder bed fusion; wear resistant materials; material properties; friction

1. Introduction

Compared with traditional subtractive manufacturing techniques, additive manufacturing is based on layer-by-layer incremental manufacturing [1]. Therefore, most additive manufacturing technologies usually use powder or wire as raw materials, which are sintered or melted by thermal focusing and then consolidated to form parts under subsequent cooling [2]. Additive manufacturing has attracted intensive attention in the past decade due to its extensive design freedom and short preparation time [3]. It has undergone more than 20 years of development [4]. Its initial goal is to rapidly fabricate porous structures and prototypes. With the advancement of the manufacturing technology of additive materials, the density and quality of parts have been improved, and it has been widely used in the medical field [5]. Today, dense parts of a variety of materials including steel, aluminum and titanium can be made by additive manufacturing techniques and [6]. Hot isostatic pressing (HIP) is used to reduce the porosity of parts and increase the density of metals and alloys. Effects of high temperature and high pressure promote the change of microstructure, beneficial phase transformation, decrease of porosity and increase of density of alloys, thus promoting their properties [7–9]. Under the joint action of isostatic pressure and increasing temperature, plastic flow occurs first, and then dispersion occurs. It has been previously reported that HIP reduces the surface porosity of casting and powder metallurgy (P/M) alloys by 24% and 68%, respectively. In the direct metal laser sintering (DMLS) process, the laser energy density is insufficient, which will make the powder materials not be completely densified. Therefore, the density and mechanical properties of DMLS parts will be improved by HIP process.

In additive manufacturing, there are two main techniques for producing metal materials [10]. One is based on metal fused deposition, such as laser melting deposition(LMD) and wire and arc additive manufacturing (WAAM) [11]. The metal deposition process melts the powder during placement. The other is based on Powder Bed Fusion (PBF), such as selective laser sintering (SLS) and DMLS. Powder sintering is the selective sintering of materials on a diffused powder (Diffusion behavior of powder material spreading on the worktable before sintering) layer according to a pre-slice computer aided design (CAD) model. Compared to fused deposited materials, powder sintered materials have higher precision, a rougher surface and lower productivity. The differences in mechanical properties and microstructure of laser sintered and laser melted aluminum alloys were compared [12]. In this paper, we only focus on SLS and DMLS.

In PBF, the laser power (usually 200 W) is concentrated at a small point less than 100 μm in diameter. The temperature inside the point can reach over 2000 °C while the temperature nearby is only a few hundred degrees, resulting in a huge thermal gradient. In addition, laser scanning speeds range from tens of thousands to thousands mm/s. As a result, parts undergo rapid and repetitive heating/cooling cycles [13,14]. The microstructure of PBF materials differs from that of materials prepared by traditional processes in terms of grain size and morphology, pores and cracks, phases and residual stresses. Different microstructures lead to different mechanical properties of the material. Many researchers have investigated the effects of different processing parameters on the microstructure and mechanical properties of materials. Gu et al. (2008) and Trelewicz et al. (2016) studied microstructure and processing parameters of DMLSed 316L stainless steel [15]; Krishnan et al. (2014) and Yan et al. (2015) studied microstructure and mechanical properties of DMLSed AlSi10Mg [16,17]; Becker et al. (2015) and Book T A et al.(2016) studied microstructure of DMLSed Ti6Al4V [18,19]; Khanna et al. (2019) studied density and surface roughness of SLSed Invar36 alloy [20]. These analyses the effects of laser processing parameters on microstructure, phase evaluation, density, hardness, tensile strength, fatigue strength, and the like.

Wear is the loss and displacement of the contact surface of the material during contact, which is an important reason for limiting the service life of the machine and causing economic losses [21,22]. According to the surface damage characteristics of the material, the wear can be divided into abrasive wear, adhesive wear, fatigue wear, and corrosion wear. The wear mechanism is highly dependent on material properties and contact conditions, including contact load, operating speed, temperature, and lubrication conditions [23–26]. In the field of industry, the research on wear is mainly the parts made by conventional technology. Before direct metal laser sintered parts are used in the industrial field, a lot of research must be done on their wear mechanism. In addition, wear and tear in orthopedic implants is difficult to replace, so wear in the biomedical field is also an important research direction. However, there are few studies on the friction and wear of PBF parts. This is because most of the PBF components are used as structural components, in which case it is more important to increase the compactness and strength of the material than to reduce wear. On the other hand, the wear resistance is independent of the density of the part. F. Martin et al. [27] found that AISI 316L with different porosity has different wear characteristics with different lubrication conditions. In the case of carboxymethyl cellulose sodium salt medium viscosity (CMC) lubricant, the wear rate decreases with the increase of porosity. Wear resistance is more dependent on application and material properties. Wear mechanism is more dependent on application and operating conditions.

This review paper summarized the research on friction and wear behavior from published articles. The purpose of this paper is to emphasize the importance of PBF part wear, thereby extending PBF technology to produce friction sub-components. Material properties of PBF components that may affect contact and wear are described. The fretting contact, sliding contact wear behaviors and mechanisms are analyzed. Finally, the future development trend is discussed.

2. Powder Bed Fusion

2.1. Process

PBF is a rapid prototyping technology that uses the laser beam to bond powder materials into three-dimensional shape. First, a new powder layer is coated on the building platform with a knife blade or roller. Then, the cross section of the component is melted by laser, as shown in Figure 1. The final step is to consolidate the powder and repeat the three steps until the components are fully formed [28]. In this process, the characteristics of parts and the adhesion between layers are mainly affected by temperature [29], the thickness of powder layer, material properties (viscosity, etc.) [30], surface tension [29], and the efficiency of laser absorption [30]. In fact, any material that can be powdered (plastics, polymers, ceramics, metals and even composites) can be formed by PBF technology [31,32]. Due to the high reflectivity and high thermal conductivity of copper, it is difficult for a one-component copper powder to form a dense sample due to excessive pores during sintering. With the development of multi-metal powders, multi-component Cu powder materials improve the sintering characteristics of Cu powders. The density and mechanical properties of the sintered copper alloy are improved. Today, laser sintered Cu alloys have found wide applications in the aerospace industry. The limitation of this method is related to the thermal properties of the powder. The powder must be kept intact and will not decompose completely during laser application.

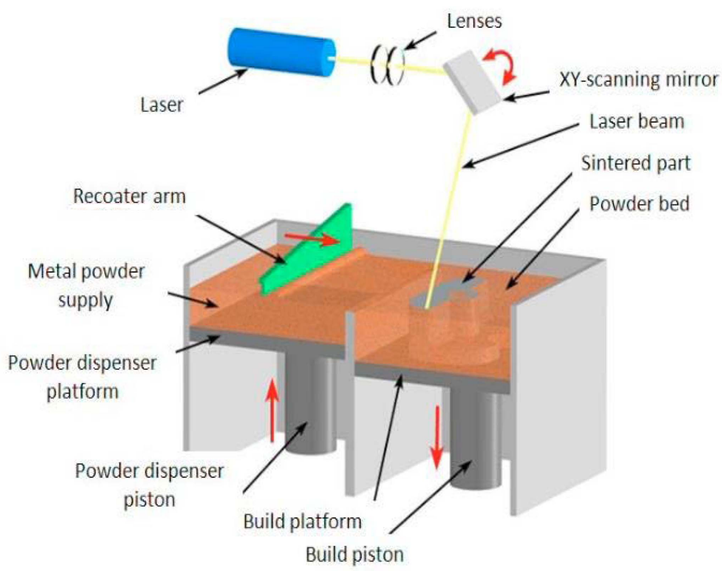

Figure 1. The selective laser sintering process, reproduced from [28], with permission from Elsevier, 2016.

2.2. Materials and Processing Parameters

Different process parameters and powder compositions have an important influence on the wear behavior of formed parts, as shown in Figure 2 [29]. According to the different properties of powder materials, it can be divided into metal powders, metal polymer powders, polymer powders and nano ceramic powders. Metal powders can be generally divided into the single metal type, the multi-component metal type and the pre alloy type. The PBF parts with single metal powders have obvious spheroidization and agglomeration. For example, PBF of single aluminum and magnesium alloy powder is much more difficult than other metal powders [33]. Due to the active chemical properties of aluminum and magnesium alloy powders and their easy oxidation, the PBF process of powder is faced with many problems, such as difficult to pave powders, easy to oxidize and splash powders, easy to spheroidize and poor surface quality of formed parts. Multi metal powders is generally composed of high melting point structural materials and low melting point binding materials. The research of multi-component metal powders focus on copper based metal powders, iron-based metal powder and nickel based metal powders [34,35]. The particle size matching and distribution of multi-component metal powders have great influence on the densification of laser sintered parts. In the PBF parts of pre alloyed powders, the liquid phase formed in the whole microstructure makes the sintering more homogeneous. The research of pre alloyed powders mainly focuses on Inconel®625, Ti6Al4V, stainless steel, high speed steel, tool steel, etc [36]. Metal polymer composite powders can be divided into mechanical mixture of metal powders and organic polymer and polymer coated metal powder. Compared with mechanical mixed powders, coated metal powders have higher strength. Polymer powder is the earliest powder material. At present, the main polymer materials used in SLS technology are thermoplastic polymer materials and their composites [37]. Because the melting point of ceramic powder is very high and the initial packing density is not high, it is difficult to sinter it. Usually, ceramic/polymer binder composite powder is prepared, and then indirect SLS is used to form ceramic materials [38,39]. The particle size distribution has an important influence on the densification of laser sintered parts. The particles with small particle size have larger specific area and smaller melting entropy, which is easy to melt in laser sintering, and has better filling effect on the gap between large particles. However, more fine particles will lead to uneven powder thickness and spheroidization in the sintering process. Figure 3 shows the relation between densification and specific energy. K is designated as the densification coefficient. Results show that different powder particle sizes and compositions have a significant effect on the density of the molding material [40].

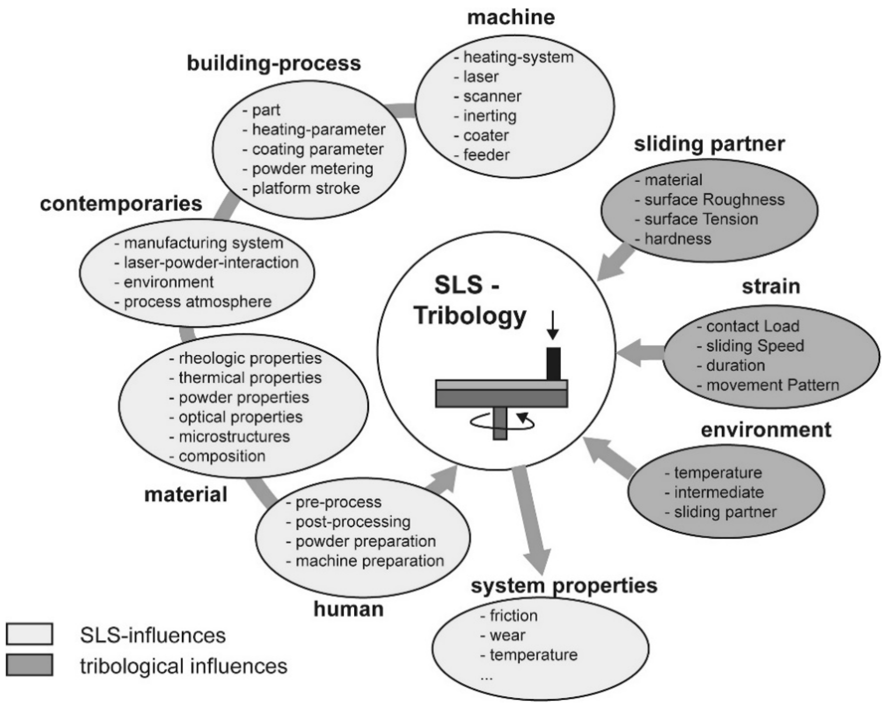

Figure 2. Factors affecting tribological properties of selective laser sintering (SLS) parts. Reproduced from [29], with permission from Elsevier, 2018.

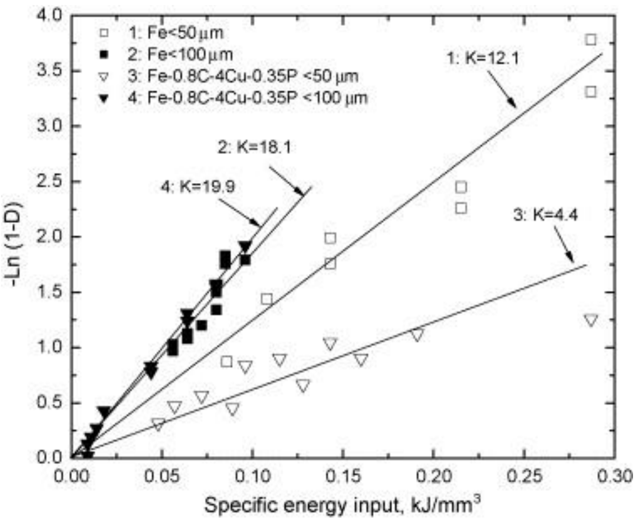

Figure 3. Effect of particle size on the densification of Fe and Fe–0.8C–4Cu–0.35P powders. Higher K value shows lower densification during direct metal laser sintering. Reproduced from [40], with permission from Elsevier, 2006.

Controlling the processing parameters can effectively improve the workpiece compactness. Machine parameters include laser power, scanning speed, scanning distance, layered distance, etc. Laser processing parameters have an important influence on the properties of materials. Sintering of powder is accomplished by laser, and the choice of scanning spacing should be related to the diameter of laser spot. Scanning speed refers to the distance traveled in unit time when laser beam scanning irradiates powder in powder bed. The scanning speed can indirectly reflect the laser energy and directly affect the forming efficiency. Every three-dimensional model is made by superimposing powder layer by layer. The thickness of superimposed powder layer by layer is the thickness of single layer. The building direction also has an important influence on the density and mechanical properties of PBF materials. The printing area and the energy density are important factors that affect the relative density of samples sintered in different directions. The energy parameters of each layer obtained by printing area and energy density can effectively control the densification of sintered parts [41,42].

3. Material Properties

As mentioned in the preamble, the material of DMLS undergoes repeated and intense heating/cooling cycles, which make the microstructure of materials different from that of traditional materials. Figure 4 shows the microstructure of the AlSi10Mg stainless steel manufactured by DMLS and traditional methods [43]. The results show that the AlSi10Mg obtained by DMLS has a finer eutectic structure than the AlSi10Mg obtained by casting. Figure 5 shows the microstructures of Ti6Al4V fabricated by DMLS and the traditional wrought process. The DMLSed Ti6Al4V alloy exhibits finer acicular α'-martensite phase [44]. Wrought Ti–6Al–4V shows an equiaxed α/β mixture and some coarse, acicular alpha phases [45]. When the material is not fully densified due to unreasonable processing parameters, pores can usually be found in the material (Figure 6) [46]. The pore size and shape are different. There are several reasons for these differences: (1) spheroidization effect [47]. Because of the high viscosity of the liquid phase, high surface tension and the fact that the melt material does not infiltrate the solid particles and matrix, spheroidization occurs in the sintering process. The appearance of spheroidization, on the one hand, will form a spherical droplet surface and a discontinuous sintering line, which will hinder the laying of the next powder layer and is not conducive to the smooth sintering process. On the other hand, there are a lot of pores in the sintering layer, which will reduce the material strength and lead to poor forming quality; (2) oxidation in the forming process. During the sintering process, the residual oxygen in the building room will combine with the powder material to form oxide, which will lead to porosity in the molding process; (3) defects of powder. Gas will remain in the powder. Since pores can negatively affect mechanical properties, researchers have made many efforts to reduce pores. Due to the existence of pores in the sample, the workpiece is prone to plastic deformation and crack growth during the wear process. Therefore, it is necessary to ensure the density of the parts during the processing to avoid voids inside the parts. On the other hand, the surface porosity of parts has a great influence on the lubrication performance and local contact conditions. Surface pores can not only store lubricating oil, improve lubrication conditions, but also facilitate the formation of lubricating films.

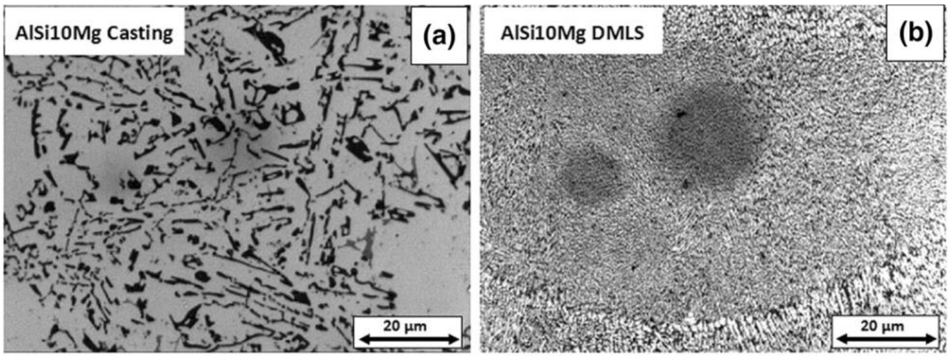

Figure 4. SEM of microstructures of 316L stainless steel produced by conventional process (**a**) and direct metal laser sintering (DMLS) (**b**). Reproduce from [43], with permission from Springer Nature, 2016.

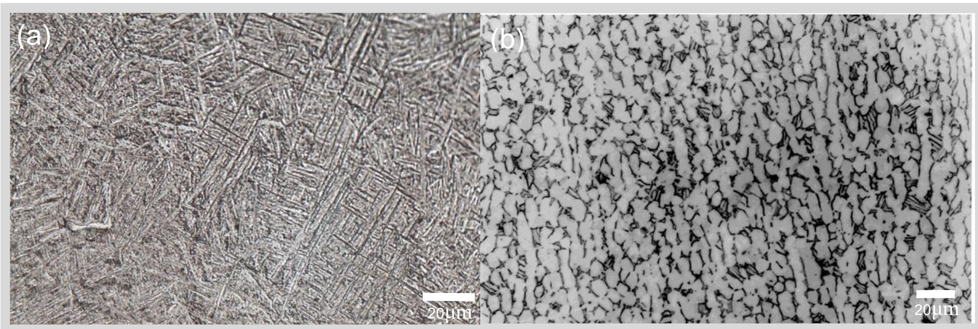

Figure 5. SEM images showing microstructures of Ti6Al4V produced by DMLS (**a**) and conventional process (**b**). Reproduced from [44,45], with permission from Elsevier, 2016 and Elsevier, 2009.

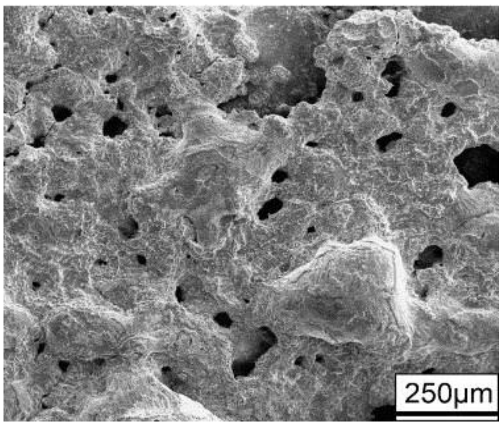

Figure 6. Pores in the W–Cu components by DMLS. Reproduced from [46]. with permission from Elsevier, 2009.

Hardness is another important factor that affects the wear properties of materials. According to the Archard equation, the hardness of a material is inversely proportional to the amount of wear.

Because of smaller grains, DMLSed materials are generally harder than materials made by traditional processes [43,48–50]. Thus, a harder DMLSed sample generally has a higher wear resistance than the materials made by traditional processes.

4. Tribological Properties

In previous studies, wear performance was often considered an integral part of the mechanical properties (such as ductility and hardness) of PBF components. Only a few studies have focused on wear behaviors and mechanisms based on specific applications.

4.1. Dry Wear

Grd et al. (2006) [51] was the first to study the wear properties of various DMLSed materials by the dry friction sliding test. The results show that the wear resistance of DMLSed materials is superior to that of traditional materials. Abrasive wear is the main cause of wear of ferronickel alloys in PBF. Table 1 lists specific dry wear contact conditions in this section.

4.1.1. Fe Alloy

Grd et al. (2006) [51] studied the friction and wear properties of DMLSed (Fe, Ni)-TiC (Figure 7) and steel fabricated by using a spherical disc experimental device. Figure 7 shows the microstructure of the sintered material. TiC particles are uniformly distributed in the Invar36 matrix. Wear resistance was improved by adding TiC. The results show that the increase of TiC content leads to the dissolution of Ti and C in the matrix of Invar36, and finally leads to the significant increase of the coefficient of thermal expansion of Invar36. At the same time, TiC has the effect of solution strengthening. In addition, Ti, as a strong BCC stabilizer, transforms the matrix FCC phase to BCC phase. Multiphase matrix strengthening may damage the ductility of materials. Figure 8 shows a typical SEM image of the worn area. The plough groove and material peeling were observed on the surface of the samples after wear, which indicated that abrasive wear was the main wear mechanism of the materials. Ramesh (2007) [52] et al. studied the friction and wear properties of materials formed under different processing parameters. The results show that the friction and wear properties of the material are related to the density and hardness of the material. Laser-molded parts sintered at lower scanning speeds have higher density and microhardness, as well as tensile strength and ductility. Because the oxide film formed by iron oxide and nitride reduces the adhesion of the material in the wear process, a lower wear rate was observed at a lower scanning speed. The experimental results show that plastic deformation and oxidation wear are the main wear mechanisms. Ramesh (2009) [53] et al. compared the tribological behavior DMLSed iron-SiC and iron. Figure 9 shows a SEM of the surface of iron and iron-SiC composites. Porosity due to unmelted powder was observed in the sintered iron. However, SiC particles are uniformly distributed in the iron composite. The wear resistance of the material was improved by adding different proportion of SiC into the powder material. With the increase of the SiC content, the hardness of the composites increases, which significantly increases the wear resistance of the composites. The higher the hardness of the composite, the better the wear resistance. Hutchings reports that the addition of hard reinforcements to soft base alloys helps to reduce abrasive wear [54]. Because the SiC particles reduce the abrasive wear of the composite material, the wear rate of iron is three times as high as that of iron-SiC (Figure 10). Naiju (2012) [55] et al. Studied the effect of processing parameters on the wear resistance of SLS iron by orthogonal test. The experimental results show that the laser power is the main factor affecting the wear of the parts. The microstructure of the sample shows that the number of pores increases with the decrease of laser power. The more pores the sample has, the easier it will wear. Amanov et al. (2013) [56] studied the tribological behavior of DMLSed Fe-Ni-Cr alloy treated hot isostatic pressing (HIP) and high-frequency ultrasonic peening (HFUP). It was found that there was no significant change in the chemical composition of HFUP treated samples. However, it can be clearly seen that the high-speed impact of the steel shot on the surface of the specimen results in spherical indentation and permanent plastic deformation, as shown in Figure 11.

The DMLSed parts treated by HFUP have higher wear resistance due to the plastic deformation of the surface, and the grain refinement and twin formation. The corrugated texture on the surface of the HFUPed part contains abrasive debris to reduce abrasive wear, which results in a lower and more stable friction coefficient (Figure 12a).The results show that the friction coefficient of the specimens treated with HFUP decreases by about 11% compared with that of the specimens not treated with HFUP (Figure 12b). HFUP-treated parts reduce plastic deformation during wear due to the increase in surface hardness, which is another important reason for reducing friction and wear.

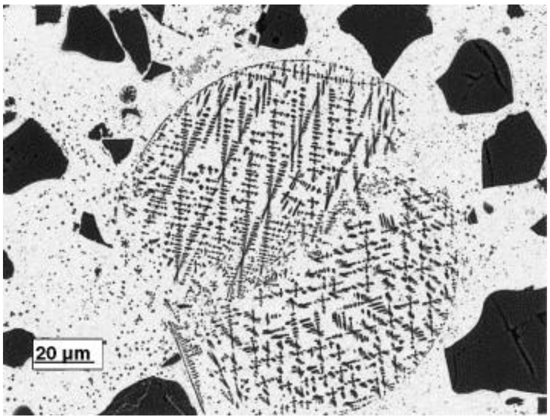

Figure 7. SEM of Invar36–30 wt.% TiC composite materials by DMLS p. Dark phase corresponds to TiC particles and bright to the Invar36 matrix. Reproduced from [51], with permission from Elsevier, 2006.

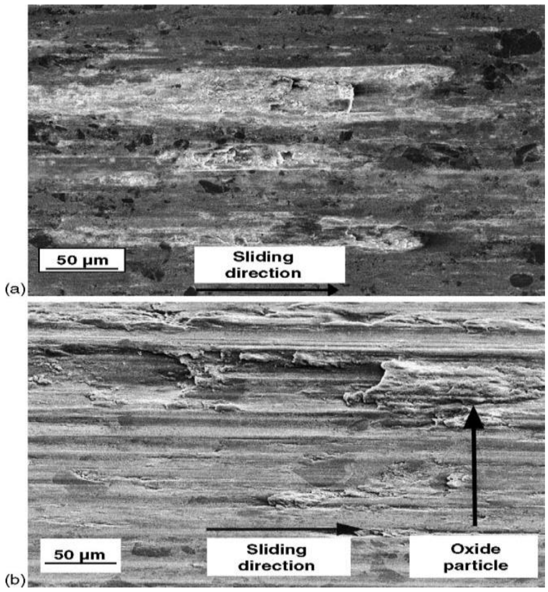

Figure 8. (**a**) Bright areas corresponds to iron oxide film on the worn surface of the Invar36–30 wt.%TiC composite. (**b**) Abrasive wear caused by iron oxide particles. Reproduced from [51], with permission from Elsevier, 2006.

Table 1. Contact conditions and wear rates under dry conditions.

Reference	DMLSed Materials/ Counterbody Material	Contact Type	Motion	Load	Speed (or Frequency)	Wear Rate (or Wear Volume)
Grd et al. (2006)	Invar36-TiC/0.12% C steel	Line	Sliding	40N	0.6 ms^{-1}	2 mm^3
Ramesh et al. (2007)	Fe/steel EN31	Point	Sliding	10–80N	0.42–3.35 ms^{-1}	1.5×10^{-4} $mm^3/N{\cdot}m$ (at laser speed 50 mm/s) 1.57×10^{-4} $mm^3/N{\cdot}m$ (at laser speed 75 mm/s) 1.75×10^{-4} $mm^3/N{\cdot}m$ (at laser speed 100 mm/s) 1.91×10^{-4} $mm^3/N{\cdot}m$ (at laser speed 125 mm/s)
Ramesh et al. (2009)	Fe-SiC Fe/SiC abrasive papers	Point	Sliding	5–25N	2.5 ms^{-1}	4.9×10^{-11} m^3/m (Fe 25N) 2.1×10^{-11} m^3/m (Fe + 1Wt.%SiC 25N) 1.8×10^{-11} m^3/m (Fe + 2Wt.%SiC 25N) 1.5×10^{-11} m^3/m (Fe + 3Wt.%SiC 25N)
Naiju et al. (2012)	Fe/steel	Point	Sliding	40N	2Hz	1.4150×10^{-12} $mm^3/N{\cdot}m$ (Layer Thickness 0.08 mm Scan Spacing 0.08 mm Laser Power 45 W) 1.2076×10^{-12} $mm^3/N{\cdot}m$ (Layer Thickness 0.08 mm Scan Spacing 0.16 mm Laser Power 50 W) 1.3272×10^{-12} $mm^3/N{\cdot}m$ (Layer Thickness 0.08 mm Scan Spacing 0.3 mm Laser Power 55 W) 1.2308×10^{-12} $mm^3/N{\cdot}m$ (Layer Thickness 0.1 mm Scan Spacing 0.08 mm Laser Power 50 W) 1.3003×10^{-12} $mm^3/N{\cdot}m$ (Layer Thickness 0.1 mm Scan Spacing 0.16 mm Laser Power 55 W) 1.6003×10^{-12} $mm^3/N{\cdot}m$ (Layer Thickness 0.1 mm Scan Spacing 0.3 mm Laser Power 45 W) 1.2848×10^{-12} $mm^3/N{\cdot}m$ (Layer Thickness 0.12 mm Scan Spacing 0.08 mm Laser Power 55 W) 1.5455×10^{-12} $mm^3/N{\cdot}m$ (Layer Thickness 0.12 mm Scan Spacing 0.16 mm Laser Power 45 W) 1.4239×10^{-12} $mm^3/N{\cdot}m$ (Layer Thickness 0.12 mm Scan Spacing 0.3 mm Laser Power 50 W)

Table 1. *Cont.*

Reference	DMLSed Materials/ Counterbody Material	Contact Type	Motion	Load	Speed (or Frequency)	Wear Rate (or Wear Volume)
Amanov et al. (2013)	Fe–Ni–Cr alloy/ steel	Point	Sliding	400 mN	8 ms^{-1}	5.25×10^{-12} m^3/N·m (HFUP-free) 4.51×10^{-12} m^3/N·m (HFUP-treated)
Lorusso et al. (2015)	AlSi10Mg/WC	Point	Sliding	5N	0.2 ms^{-1}	1.39×10^{-2} mm^3/m (AlSi10Mg Casting) 9×10^{-3} mm^3/m (AlSi10Mg DMLS) 2.05×10^{-2} mm^3/m (AlSi10Mg/uTiB_2) 7×10^{-3} mm^3/m (AlSi10Mg/nano TiB_2)
Ghosh et al. (2011)	Al-SiC/WC-Co	Point	Sliding	4.9 N	0.063 ms^{-1}	1.62×10^{-4} mm^3/N·m (10Wt.%SiC) 1.1×10^{-4} mm^3/N·m (15Wt.%SiC) 0.7×10^{-4} mm^3/N·m (20Wt.%SiC) 0.68×10^{-4} mm^3/N·m (25Wt.%SiC) 0.64×10^{-4} mm^3/N·m (30Wt.%SiC)
Chandramohan et al. (2018)	Ti6Al4V/steel	Point	Sliding	5N 15N 25N	No data	0.97 mm^3 (Sintered-HB 15N) 1.13 mm^3 (Sintered-VB 15N) 0.61 mm^3 (HT1-HB 15N) 0.45 mm^3 (HT1-VB 15N) 0.4 mm^3 (HT2-HB 15N) 0.29 mm^3 (HT2-VB 15N)
Chandramohan et al. (2017)	Ti6Al4V/steel	Point	Sliding	5N 15N 25N	No data	0.89 mm^3 (HB 5N) 1.34 mm^3 (VB1 5N) 1.26 mm^3 (VB2 5N) 1.32 mm^3 (VB3 5N) 1.3 mm^3 (VB4 5N) 1.09 mm^3 (VB5 5N)
Patil et al. (2019)	Ti6Al4V/ steel EN31	Point	Sliding	50N	2 ms^{-1}	0.6 μm/s (Ti6Al4V) 0.48 μm/s (Ti6Al4V + 0.5Wt.%TiB_2) 0.44 μm/s (Ti6Al4V + 1Wt.%TiB_2) 0.42 μm/s (Ti6Al4V + 2Wt.%TiB_2)

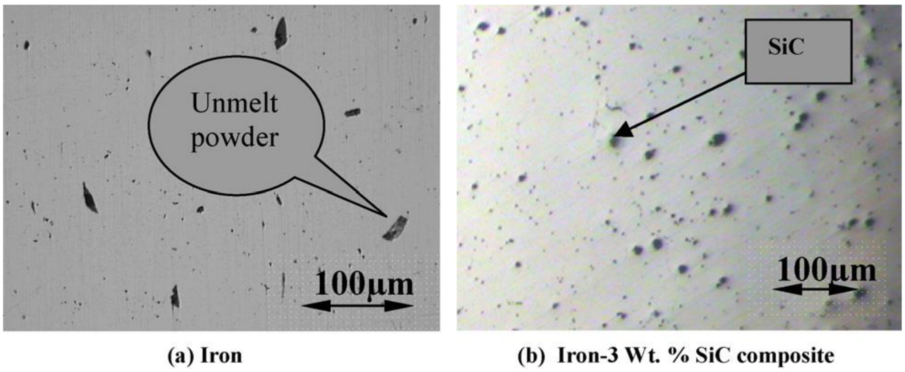

Figure 9. (**a**,**b**) SEM of iron and iron–SiC composites (sintered at laser speed of 100 mm/s). Reproduced from [53], with permission from Elsevier, 2009.

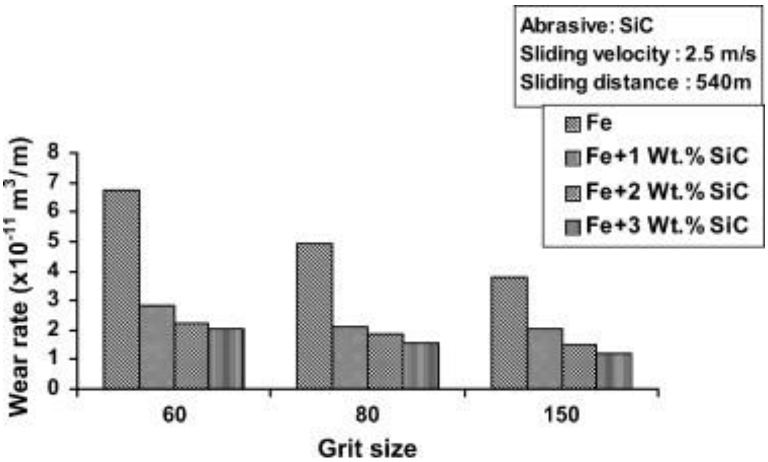

Figure 10. Wear rate of iron and iron-SiC composites. Reproduced from [53], with permission from Elsevier, 2009.

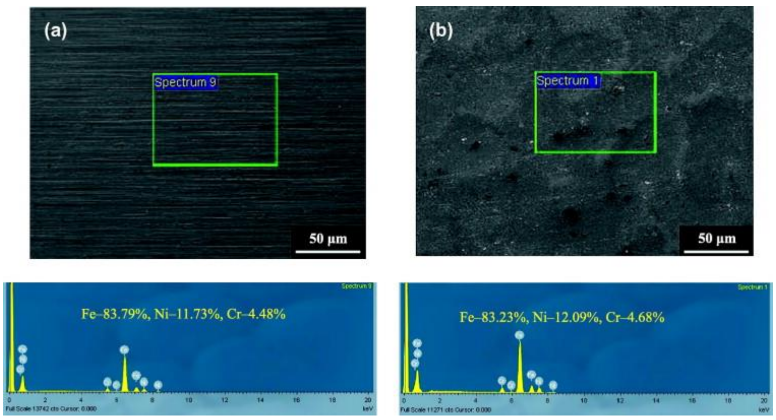

Figure 11. SEM and X-ray energy spectrum analysis (EDS) analyses of the high-frequency ultrasonic peening (HFUP)-free (**a**) and HFUP-treated (**b**) specimens. Reproduced from [56], with permission from Elsevier, 2013.

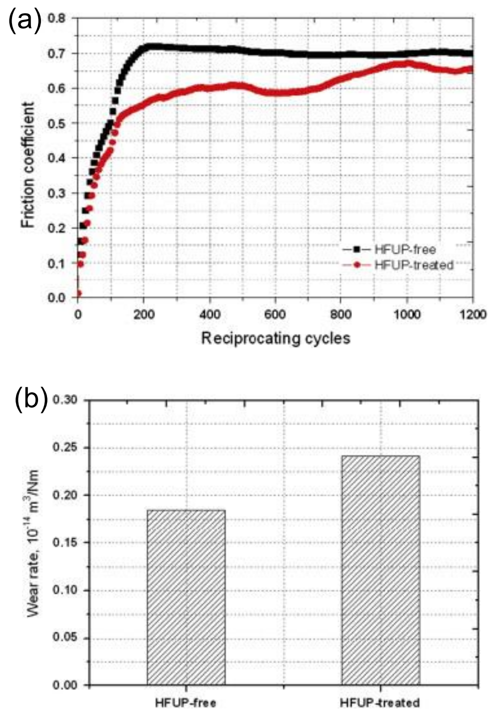

Figure 12. Comparison of average friction coefficient (**a**) wear rate (**b**) of the ball counter surfaces slid against the HFUP free and HFUP-treated specimens. Reproduced from [56], with permission from Elsevier, 2013.

4.1.2. Al Alloy

Ghosh et al. (2011) [57] investigated the friction and wear behavior of SiC particulate (SiCp) reinforced Al-based metal matrix composites (Al-MMC) (92.5 wt.% of Al, 4.5 wt.% of Cu, 3 wt.% Mg) under the ball-disk contact condition. The results show that the harder SiC particles bear most of the contact stress during the wear process, hindering the plastic deformation of the surface materials, and greatly increasing the wear resistance of the composites (Figure 13). Fragmented SiC particulates can also cause abrasive wear. Lorusso et al. (2016) [43] investigated the friction and wear properties of DMLSed AlSi10Mg-TiB_2 by sliding contact. The mechanical properties of DMLS specimens with different proportion of TiB_2 in AlSi10Mg were tested. Microhardness tests show that AlSi10Mg/TiB2 has higher hardness than AlSi10Mg Casting, as shown in Figure 14. The results show that with the introduction of the second term, the yield strength and ultimate strength of the parts decrease, while the elongation and Young's modulus increase. The results of the sliding wear test show that the TiB2 added AlSi10Mg has a significantly reduced friction coefficient because the detached TiB2 particles act as solid lubricants at the contact interface during the wear process. Due to the finer microstructure of DMLSed AlSi10Mg, which shows higher hardness and better mechanical properties, the wear of DMLSed AlSi10Mg is lower than that of cast AlSi10Mg alloy (Figure 15). The wear mechanism of DMLSed AlSi10Mg and cast AlSi10Mg is abrasive wear, while the wear mechanism of AlSi10Mg with TiB2 is delamination.

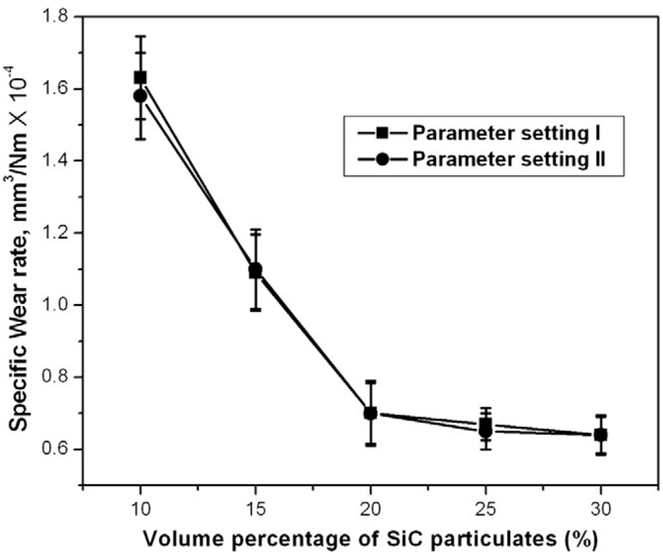

Figure 13. Graphical representation of specific wear rate vs. vol.% of SiCp variation. Reproduced from [57], with permission from Elsevier, 2011.

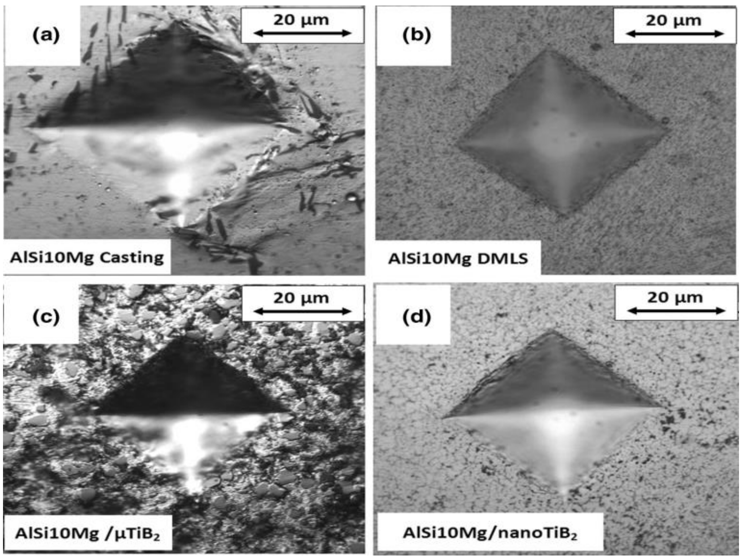

Figure 14. The microhardness indentations on AlSi10Mg samples obtained by casting (**a**) and DMLS (**b**), and of the composites with micro- (**c**) and nano TiB2 particles (**d**). Reproduced from [43], with permission from Springer Nature, 2016.

4.1.3. Ti and Titanium Alloy

Chandramohan et al. (2017) [58] studied the friction and wear properties of DMLSed Ti6Al4V materials with different building directions (HB-horizontal built and VB-vertical built) after heat treatment (HT). Martensite was found in the β-phase matrix in the sintered Ti–6Al–4V microstructure, as shown in Figure 16. The experimental results show that the grain refinement after heat treatment can effectively increase the wear resistance of the material. There are dense oxide debris on the surface after heat treatment. Compact oxide debris can lubricate the worn surface, which can reduce the wear of the material and improve the wear resistance of the material significantly. The sintered and heat-treated samples are both typical abrasive wear and adhesive wear mechanisms, and the oxidative wear after heat treatment significantly reduces the wear rate. The influence of heat treatment on wear resistance of DMLSed parts is more important than the direction of building (Figure 17) [59,60]. Chandramohan et al. (2018) [5] studied the friction and wear properties of Ti6Al4V samples in different building directions (HB-horizontal built and VB-vertical built). The experimental results show that martensite is present in the vertically constructed sample, while the horizontally constructed sample consists of mixed alpha and beta phases. As shown in Figure 18, since the specimen of the vertical structure has higher hardness, which reduces abrasive wear and adhesive wear during abrasion, it has better wear resistance under high stress. Oxidation wear is an important reason for the low wear rate of the alloy. Patil et al. (2019) [61] investigated the friction behavior of DMLSed Ti6Al4V with addition of varying amount of TiB2 on pin-on-disk tribometer. The uniformly dispersed TiB strengthens the Ti6Al4V alloy, which refines the grains and improves the hardness. The increase in hardness improves the plastic deformation resistance of the alloy and reduces abrasive wear.

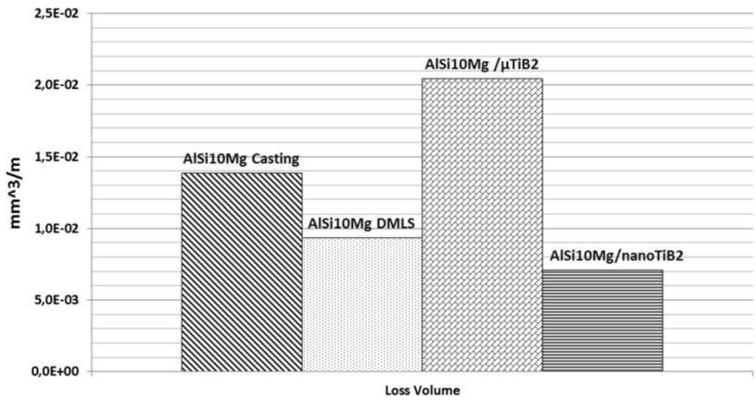

Figure 15. Volume per meter loss after wear tests of the AlSi10Mg samples obtained by casting and DMLS, and of the composites with micro- and nano TiB_2 particles. Reproduced from [43], with permission from Springer Nature, 2016.

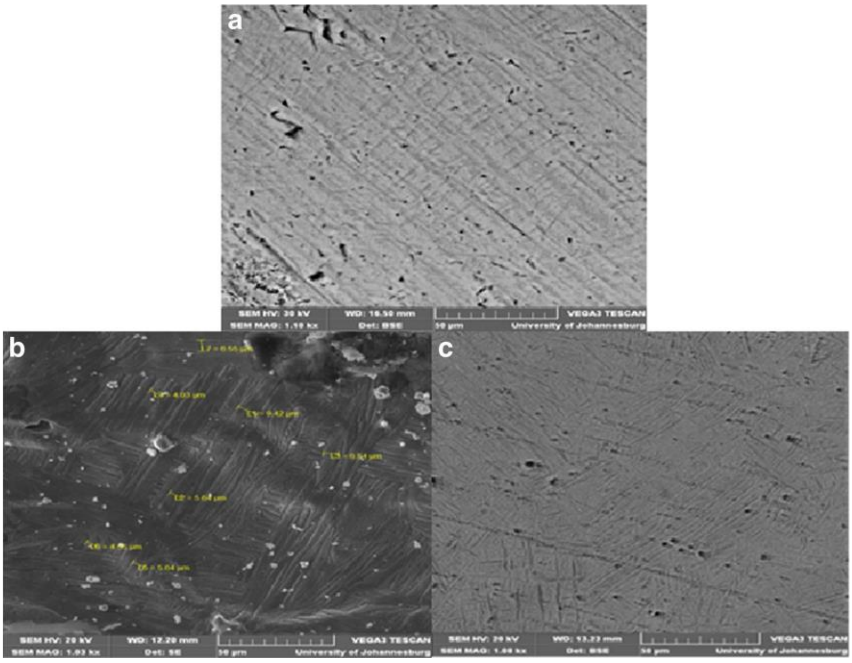

Figure 16. Microstructures of (**a**) sintered VB, (**b**) HT 1-VB and (**c**) HT 2-VB. Reproduced from [58], with permission from Springer Nature, 2017.

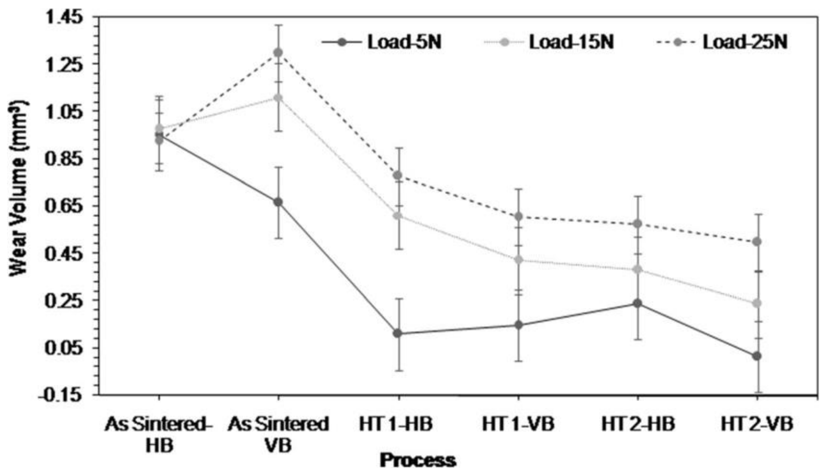

Figure 17. Wear volume of assintered and heat-treated specimens. Reproduced from [58], with permission from Springer Nature, 2017.

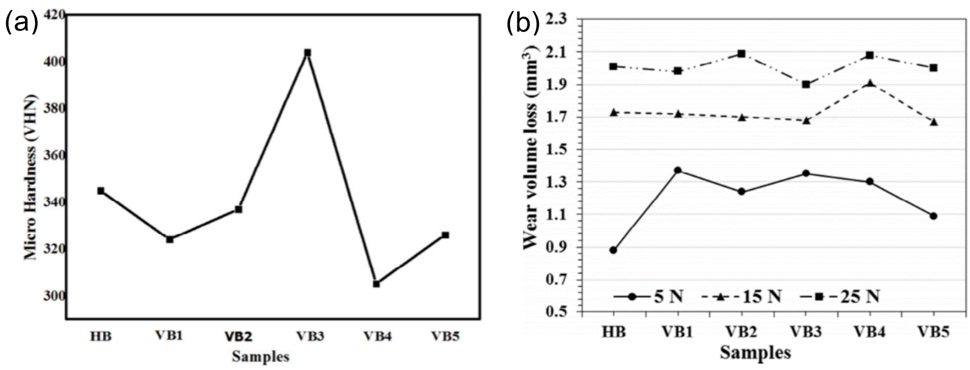

Figure 18. (**a**) Microhardness of horizontal and vertical built specimens, (**b**) Wear performance of horizontal and vertical built specimens. Reproduced from [5], with permission from Elsevier, 2018.

4.2. Fretting Wear

Fretting wear is a wear phenomenon caused by the relative oscillation of small displacement amplitude between two contact interfaces in tangential motion [62–66]. The PBF technology has been widely used in the medical field, mainly in the manufacture of artificial joints, artificial bones and so on. Fretting wear of artificial joints is an important reason to limit their service life, but there are few studies on fretting wear of SLSed materials. Kumar et al. (2008) [32] (2008) was the first to studied the friction and wear of SLS steel under fretting condition by spherical contact. It is found that the wear resistance of SLS steels is superior to that of the materials manufactured by traditional processes because of the addition of friction-friendly elements such as copper. The results show that the main wear mechanism of stainless steels is abrasive wear and adhesive wear. Kumar et al. (2009) [67] then carried out friction and wear experiments under fretting condition by adding WC-Co to tool steel. The results showed that the sintered material with WC-Co had higher hardness and strength, and had better wear resistance than tool steel manufactured by traditional process. The experimental results show that the main wear mechanism of steel is adhesive wear (Figure 19). Kumar et al. (2008) [68] compared the friction and wear properties of steel manufactured by SLS and traditional process under fretting condition by means of elastic contact. It is found that although the steel prepared by traditional process has higher hardness, its wear rate is higher than that of SLS steel.

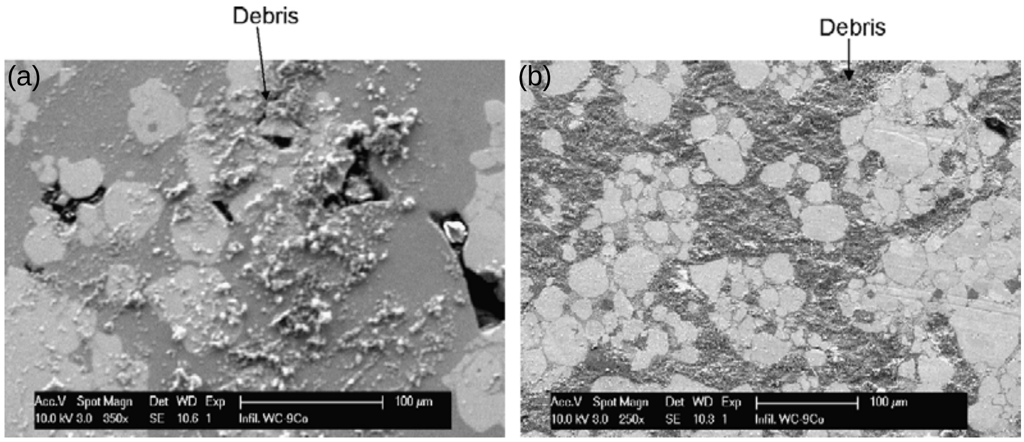

Figure 19. Micrographs of infiltrated WC 9Co samples after fretting tests (**a**) load 2N, (**b**) load 4N. Reproduced from [67], with permission from Elsevier, 2009.

4.3. Sliding Wear under Lubricated Conditions

In order to reduce friction and wear of parts, most industrial parts are in the lubrication state in actual working conditions. Under the lubrication condition, the friction behavior of parts with pore and cracks is different from that of parts under dry friction condition. At present, there are few researches on the wear behavior of PBFmaterials under lubrication. At the same time, the current research content is not deep enough to reveal the wear mechanism of sintered parts under lubrication. Naiju et al. (2014) [69] studied the effects of load, temperature and hardness on the wear properties of DMLSed bronze under oil lubrication. The results show that compared with temperature and hardness, the effect of load on wear properties of materials is more significant. Naiju et al. et al. (2018) [70] subsequently prepared bronze alloys by mixing metal and polymer powders. The effect of temperature on the friction and wear properties of the samples under oil lubrication was studied. It is found that the wear rate increases with the increase of temperature. It is also found that material defects such as cavity, segregation and hot crack will affect the wear rate. The parts with pore also show certain wear resistance. Oxidation wear is the main wear mechanism.

5. Discussion, Future Work, and Concluding Remarks

From the above literature review, it can be seen that most of the research is carried out under dry friction conditions. Contact forms include points, lines and surfaces. The sliding speeds vary from 0.42 to 2.5 m/s. The friction and wear properties of PBF parts were studied under such extensive contact conditions. It can be seen that the wear resistance of PBF parts is better than that of traditional parts. The processing parameters of PBF have a great influence on the density, hardness and wear rate of the material. Researchers generally believe that the reasonable process parameters of PBF can improve the compactness of materials and further improve the wear resistance of parts under dry friction conditions. PBF materials that are completely densified due to the small and closely arranged grains have higher resistance to deformation than materials made by traditional processes. On the other hand, reasonable processing parameters can refine the grains and increase the hardness of the material, which is an important factor for the material to have higher wear resistance.

Due to the strengthening effect of the second phase on the matrix, the addition of different proportions of second phase particles into the powder has also attracted the attention of researchers. Reasonable addition of second phase particles can effectively improve the wear resistance of the alloy. In their research work, the poor compactness of PBF parts results in the appearance of voids, which affects the wear resistance of parts. Poor compactness will lead to voids and cracks in parts, which will further expand under harsh contact conditions, leading to material delamination and high wear.

However, most of the friction pairs are used in lubrication. At present, the research on the wear of PBF parts focused on dry friction cannot fully adapt to the current application environment of all friction pairs. The research on friction behaviors of PBF parts under lubrication in the literature pays more attention to the influence of loads, temperatures and other test conditions. However, little research has been done on the lubrication state, the role of lubricants and the influence of wear interface under the lubrication state. It is found that material defects such as cavity, segregation and hot crack can affect wear rate. Components with interconnected cavity networks have higher wear rates. Therefore, this part of the existing research cannot help us correctly understand the friction and wear properties and wear mechanism of PBF parts under lubrication. At the same time, little research has been done on the effect of all or part of the formation of lubricating oil film on the wear of parts. In this case, the influence of lubrication film may exceed that of the microstructure of PBF parts. Surface voids have a positive effect on the formation of lubrication film, but voids will reduce the impact of compactness on the friction and wear properties of parts. Nowadays, the focus of extensive research is on surface texture. The textured surface can store lubricating oil and debris under lubrication, which can effectively reduce friction and wear. Whether pore has a positive effect on reducing friction and wear is a problem to be solved. It can be seen from the literature review that different combinations of PBF process parameters may cause porosity in parts. The interaction between pore and its counterpart (or lubricating film) under different contact conditions is worth studying. Finally, by adjusting the process parameters of PBF and actively controlling the porosity and microstructure of PBF materials, the purpose of low friction and wear is achieved.

Fretting wear is an important cause of damage in artificial joints and artificial bones. PBF is one of the main technologies for the production of artificial joints and artificial bones. However, there are few studies on this aspect. The existing studies have found that the materials prepared by PBF have a better wear resistance than those prepared by traditional processes under fretting wear conditions. This provides an important basis for the application of PBF in the medical field. However, the current research on fretting wear forms and contact conditions is also very inadequate. At present, the fretting modes studied are only limited to tangential fretting in point-to-surface contact, but there are various fretting modes of parts in actual operation. It is of great value to study fretting forms closer to actual working conditions for the application of PBF. Artificial bone is widely used in organic soluble environment. However, the current research is limited to dry friction conditions. It is very important to study the material of PBF under different lubrication conditions.

In conclusion, the wear of PBF materials under dry friction, boundary lubrication and fretting conditions has been extensively studied. The processing parameters of PBF are very important for the reduction of the wear rate, because fully compact parts usually have a high wear resistance. Different powder materials have significant influence on the wear resistance of parts after forming. However, from dry friction conditions to different lubrication conditions, the effect of pore on deformation and lubrication behavior remains to be further studied. More importantly, it is necessary to understand the mechanism behind the wear behavior of PBF parts. Through different wear mechanism, different laser sintering methods are adopted, and then PBF process parameters and powder composition are actively controlled to improve the wear resistance of parts. In this case, the application of PBF technology can be greatly extended to the manufacture of friction pairs.

Author Contributions: Conceptualization, W.L.; investigation, H.Q., W.L., R.X. and J.W.; writing—original draft preparation, H.Q., R.X. and W.L.; writing—review and editing, P.L., H.Q. and W.L.; All authors have read and agreed to the published version of the manuscript.

Funding: This project is supported by National Natural Science Foundation of China (No. 51975325).

Conflicts of Interest: The authors declare no conflict of interest.

References

1. Emmelmann, C.; Kranz, J.; Herzog, D.; Wycisk, E. Laser additive manufacturing of metals. In *Laser Technology in Biomimetics*; Springer: Berlin, Germany, 2013; pp. 143–162.
2. Ciocca, L.; Fantini, M.; De Crescenzio, F.; Corinaldesi, G.; Scotti, R. Direct metal laser sintering (DMLS) of a customized titanium mesh for prosthetically guided bone regeneration of atrophic maxillary arches. *Med. Biol. Eng. Comput.* **2011**, *49*, 1347–1352. [CrossRef]
3. Kranz, J.; Herzog, D.; Emmelmann, C. Design guidelines for laser additive manufacturing of lightweight structures in TiAl6V4. *J. Laser Appl.* **2015**, *27*, S14001. [CrossRef]
4. Horvath, J. A brief history of 3D printing. In *Mastering 3D Printing*; Springer: Berlin, Germany, 2014; pp. 3–10.
5. Palanisamy, C.; Bhero, S.; Obadele, B.A.; Olubambi, P.A. Effect of build direction on the microhardness and dry sliding wear behaviour of laser additive manufactured Ti-6Al-4V. *Mater. Today Proc.* **2018**, *5*, 397–402. [CrossRef]
6. Murr, L.E.; Gaytan, S.M.; Ramirez, D.A.; Martinez, E.; Hernandez, J.; Amato, K.N.; Shindo, P.W.; Medina, F.R.; Wicker, R.B. Metal fabrication by additive manufacturing using laser and electron beam melting technologies. *J. Mater. Sci. Technol.* **2012**, *28*, 1–14. [CrossRef]
7. Chen, H.; Pfender, E.; Heberlein, J. Structural changes in plasma-sprayed ZrO_2 coatings after hot isostatic pressing. *Thin Solid Films* **1997**, *293*, 227–235. [CrossRef]
8. Khor, K.; Gu, Y. Hot isostatic pressing of plasma sprayed yttria-stabilized zirconia. *Mater. Lett.* **1998**, *34*, 263–268. [CrossRef]
9. Kuribayashi, H.; Suganuma, K.; Miyamoto, Y.; Koizumi, M. Effects of HIP treatment on plasma-sprayed ceramic coating onto strainless steel. *Am. Ceram. Soc. Bull.* **1986**, *65*, 1306–1310.
10. Kruth, J.-P.; Vandenbroucke, B.; Van Vaerenbergh, J.; Mercelis, P. Benchmarking of different SLS/SLM processes as rapid manufacturing techniques. In Proceedings of the International Conference Polymers & Moulds Innovations PMI 2005, Ghent, Belgium, 20–24 April 2005.
11. Sun, Y.; Moroz, A.; Alrbaey, K. Sliding wear characteristics and corrosion behaviour of selective laser melted 316L stainless steel. *J. Mater. Eng. Perform.* **2014**, *23*, 518–526. [CrossRef]
12. Olakanmi, E.O.; Cochrane, R.; Dalgarno, K. A review on selective laser sintering/melting (SLS/SLM) of aluminium alloy powders: Processing, microstructure, and properties. *Prog. Mater. Sci.* **2015**, *74*, 401–477. [CrossRef]
13. Zhu, H.; Lu, L.; Fuh, J. Development and characterisation of direct laser sintering Cu-based metal powder. *J. Mater. Process. Technol.* **2003**, *140*, 314–317. [CrossRef]
14. Bourell, D.L.; Marcus, H.L.; Barlow, J.W.; Beaman, J.J. Selective laser sintering of metals and ceramics. *Int. J. Powder Metall.* **1992**, *28*, 369–381.
15. Gu, D.; Shen, Y. Processing conditions and microstructural features of porous 316L stainless steel components by DMLS. *Appl. Surf. Sci.* **2008**, *255*, 1880–1887. [CrossRef]
16. Krishnan, M.; Atzeni, E.; Canali, R.; Calignano, F.; Manfredi, D.; Ambrosio, E.P.; Iuliano, L. On the effect of process parameters on properties of AlSi10Mg parts produced by DMLS. *Rapid Prototyp. J.* **2014**, *6*, 449–458. [CrossRef]
17. Yan, C.; Hao, L.; Hussein, A.; Young, P.; Huang, J.; Zhu, W. Microstructure and mechanical properties of aluminium alloy cellular lattice structures manufactured by direct metal laser sintering. *Mater. Sci. Eng. A* **2015**, *628*, 238–246. [CrossRef]
18. Becker, T.H.; Beck, M.; Scheffer, C. Microstructure and mechanical properties of direct metal laser sintered Ti-6Al-4V. *S. Afr. J. Ind. Eng.* **2015**, *26*, 1–10. [CrossRef]
19. Book, T.A.; Sangid, M.D. Strain localization in Ti-6Al-4V Widmanstätten microstructures produced by additive manufacturing. *Mater. Charact.* **2016**, *122*, 104–112. [CrossRef]
20. Khanna, N.; Mistry, S.; Rashid, R.R.; Gupta, M.K. Investigations on density and surface roughness characteristics during selective laser sintering of Invar-36 alloy. *Mater. Res. Express* **2019**, *6*, 086541. [CrossRef]
21. Zhai, W.; Lu, W.; Zhang, P.; Zhou, M.; Liu, X.; Zhou, L. Microstructure, mechanical and tribological properties of nickel-aluminium bronze alloys developed via gas-atomization and spark plasma sintering. *Mater. Sci. Eng. A* **2017**, *707*, 325–336. [CrossRef]

22. Zhai, W.; Shi, X.; Yang, K.; Huang, Y.; Zhou, L.; Lu, W. Tribological Behaviors of Ni_3Al Intermetallics with MoO_3 Multilayer Ribbon Crystal Prepared by Spark Plasma Sintering. *Acta Metall. Sin. (Engl. Lett.)* **2017**, *30*, 576–584. [CrossRef]
23. Thapliyal, S.; Dwivedi, D.K. Study of the effect of friction stir processing of the sliding wear behavior of cast NiAl bronze: A statistical analysis. *Tribol. Int.* **2016**, *97*, 124–135. [CrossRef]
24. Lan, P.; Meyer, J.L.; Economy, J.; Polycarpou, A.A. Unlubricated tribological performance of aromatic thermosetting polyester (ATSP) coatings under different temperature conditions. *Tribol. Lett.* **2016**, *61*, 10. [CrossRef]
25. Cai, Z.-B.; Zhu, M.-H.; Zheng, J.-F.; Jin, X.-S.; Zhou, Z.-R. Torsional fretting behaviors of LZ50 steel in air and nitrogen. *Tribol. Int.* **2009**, *42*, 1676–1683. [CrossRef]
26. Archard, J.; Rowntree, R. The temperature of rubbing bodies; part 2, the distribution of temperatures. *Wear* **1988**, *128*, 1–17. [CrossRef]
27. Martin, F.; García, C.; Blanco, Y. Influence of residual porosity on the dry and lubricated sliding wear of a powder metallurgy austenitic stainless steel. *Wear* **2015**, *328*, 1–7. [CrossRef]
28. Duda, T.; Raghavan, L.V. 3D metal printing technology. *IFAC-PapersOnLine* **2016**, *49*, 103–110. [CrossRef]
29. Wörz, A.; Dru mmer, D. Tribological anisotropy of selective laser sintered PA12 parts. *Polym. Test.* **2018**, *70*, 117–126. [CrossRef]
30. Wegner, A. *Theorie über Die Fortführung von Aufschmelzvorgängen als Grundvoraussetzung für eine Robuste Prozessführung Beim Laser-Sintern von Thermoplasten*; Universitätsbibliothek Duisburg-Essen: Duisburg, Germany, 2015.
31. Williams, J.M.; Adewunmi, A.; Schek, R.M.; Flanagan, C.L.; Krebsbach, P.H.; Feinberg, S.E.; Hollister, S.J.; Das, S. Bone tissue engineering using polycaprolactone scaffolds fabricated via selective laser sintering. *Biomaterials* **2005**, *26*, 4817–4827. [CrossRef]
32. Kumar, S.; Kruth, J.P. Wear performance of SLS/SLM materials. *Adv. Eng. Mater.* **2008**, *10*, 750–753. [CrossRef]
33. Louvis, E.; Fox, P.; Sutcliffe, C.J. Selective laser melting of aluminium components. *J. Mater. Process. Technol.* **2011**, *211*, 275–284. [CrossRef]
34. Zhu, H.; Fuh, J.; Lu, L. Microstructural evolution in direct laser sintering of Cu-based metal powder. *Rapid Prototyp. J.* **2005**, *11*, 74–81. [CrossRef]
35. Simchi, A.; Pohl, H. Direct laser sintering of iron–graphite powder mixture. *Mater. Sci. Eng. A* **2004**, *383*, 191–200. [CrossRef]
36. Das, S.; Wohlert, M.; Beaman, J.J.; Bourell, D.L. Processing of titanium net shapes by SLS/HIP. *Mater. Des.* **1999**, *20*, 115–121. [CrossRef]
37. Zhu, W.; Yan, C.; Shi, Y.; Wen, S.; Liu, J.; Shi, Y. Investigation into mechanical and microstructural properties of polypropylene manufactured by selective laser sintering in comparison with injection molding counterparts. *Mater. Des.* **2015**, *82*, 37–45. [CrossRef]
38. Harlan, N.R.; Bourell, D.L.; Beaman, J.J.; Reyes, R. Titanium castings using laser-scanned data and selective laser-sintered zirconia molds. *J. Mater. Eng. Perform.* **2001**, *10*, 410–413. [CrossRef]
39. Shahzad, K.; Deckers, J.; Boury, S.; Neirinck, B.; Kruth, J.-P.; Vleugels, J. Preparation and indirect selective laser sintering of alumina/PA microspheres. *Ceram. Int.* **2012**, *38*, 1241–1247. [CrossRef]
40. Simchi, A. Direct laser sintering of metal powders: Mechanism, kinetics and microstructural features. *Mater. Sci. Eng. A* **2006**, *428*, 148–158. [CrossRef]
41. Ponnusamy, P.; Masood, S.; Ruan, D.; Palanisamy, S.; Rashid, R. High strain rate dynamic behaviour of AlSi12 alloy processed by selective laser melting. *Int. J. Adv. Manuf. Technol.* **2018**, *97*, 1023–1035. [CrossRef]
42. Rashid, R.; Masood, S.; Ruan, D.; Palanisamy, S.; Rashid, R.R.; Elambasseril, J.; Brandt, M. Effect of energy per layer on the anisotropy of selective laser melted AlSi12 aluminium alloy. *Addit. Manuf.* **2018**, *22*, 426–439. [CrossRef]
43. Lorusso, M.; Aversa, A.; Manfredi, D.; Calignano, F.; Ambrosio, E.P.; Ugues, D.; Pavese, M. Tribological behavior of aluminum alloy AlSi10Mg-TiB_2 composites produced by direct metal laser sintering (DMLS). *J. Mater. Eng. Perform.* **2016**, *25*, 3152–3160. [CrossRef]
44. Konečná, R.; Kunz, L.; Bača, A.; Nicoletto, G. Long fatigue crack growth in Ti6Al4V produced by direct metal laser sintering. *Procedia Eng.* **2016**, *160*, 69–76. [CrossRef]

45. Murr, L.; Esquivel, E.; Quinones, S.; Gaytan, S.; Lopez, M.; Martinez, E.; Medina, F.; Hernandez, D.; Martinez, E.; Martinez, J. Microstructures and mechanical properties of electron beam-rapid manufactured Ti–6Al–4V biomedical prototypes compared to wrought Ti–6Al–4V. *Mater. Charact.* **2009**, *60*, 96–105. [CrossRef]
46. Gu, D.; Shen, Y. Effects of processing parameters on consolidation and microstructure of W–Cu components by DMLS. *J. Alloys Compd.* **2009**, *473*, 107–115. [CrossRef]
47. Gu, D.; Shen, Y. Balling phenomena in direct laser sintering of stainless steel powder: Metallurgical mechanisms and control methods. *Mater. Des.* **2009**, *30*, 2903–2910. [CrossRef]
48. Barucca, G.; Santecchia, E.; Majni, G.; Girardin, E.; Bassoli, E.; Denti, L.; Gatto, A.; Iuliano, L.; Moskalewicz, T.; Mengucci, P. Structural characterization of biomedical Co–Cr–Mo components produced by direct metal laser sintering. *Mater. Sci. Eng. C* **2015**, *48*, 263–269. [CrossRef]
49. Lapcevic, A.R.; Jevremovic, D.P.; Puskar, T.M.; Williams, R.J.; Eggbeer, D. Comparative analysis of structure and hardness of cast and direct metal laser sintering produced Co-Cr alloys used for dental devices. *Rapid Prototyp. J.* **2016**, *22*, 144–151. [CrossRef]
50. Asgari, H.; Moha mmadi, M. Microstructure and mechanical properties of stainless steel CX manufactured by Direct Metal Laser Sintering. *Mater. Sci. Eng. A* **2018**, *709*, 82–89. [CrossRef]
51. Gåård, A.; Krakhmalev, P.; Bergström, J. Microstructural characterization and wear behavior of (Fe, Ni)–TiC MMC prepared by DMLS. *J. Alloys Compd.* **2006**, *421*, 166–171. [CrossRef]
52. Ramesh, C.; Srinivas, C.; Srinivas, K. Friction and wear behaviour of rapid prototype parts by direct metal laser sintering. *Tribol. Mater. Surf. Interfaces* **2007**, *1*, 73–79. [CrossRef]
53. Ramesh, C.; Srinivas, C.; Channabasappa, B. Abrasive wear behaviour of laser sintered iron–SiC composites. *Wear* **2009**, *267*, 1777–1783. [CrossRef]
54. Hutchings, I. Tribological properties of metal matrix composites. *Mater. Sci. Technol.* **1994**, *10*, 513–517. [CrossRef]
55. Naiju, C.; Manoj, P.; George, T.T.; Kurian, J. Study on the Effect of Process Parameters on Reciprocating Wear Behavior of Components Produced by Selective Laser Sintering (SLS). *Adv. Mater. Res.* **2012**, *488*, 1424–1428. [CrossRef]
56. Amanov, A.; Sasaki, S.; Cho, I.-S.; Suzuki, Y.; Kim, H.-J.; Kim, D.-E. An investigation of the tribological and nano-scratch behaviors of Fe–Ni–Cr alloy sintered by direct metal laser sintering. *Mater. Des.* **2013**, *47*, 386–394. [CrossRef]
57. Ghosh, S.K.; Saha, P. Crack and wear behavior of SiC particulate reinforced aluminium based metal matrix composite fabricated by direct metal laser sintering process. *Mater. Des.* **2011**, *32*, 139–145. [CrossRef]
58. Chandramohan, P.; Bhero, S.; Obadele, B.A.; Olubambi, P.A. Laser additive manufactured Ti–6Al–4V alloy: Tribology and corrosion studies. *Int. J. Adv. Manuf. Technol.* **2017**, *92*, 3051–3061. [CrossRef]
59. Yao, J.; Suo, T.; Zhang, S.; Zhao, F.; Wang, H.; Liu, J.; Chen, Y.; Li, Y. Influence of heat-treatment on the dynamic behavior of 3D laser-deposited Ti–6Al–4V alloy. *Mater. Sci. Eng. A* **2016**, *677*, 153–162. [CrossRef]
60. Lahiri, I.; Lahiri, D.; Bhargava, S. Effect of Prior β Processing on Superplasticity of (α + β) Thermomechanically Treated Ti–6Al–4V Alloy. *Mater. Manuf. Process.* **2003**, *18*, 621–635. [CrossRef]
61. Patil, A.S.; Hiwarkar, V.D.; Verma, P.K.; Khatirkar, R.K. Effect of TiB2 addition on the microstructure and wear resistance of Ti-6Al-4V alloy fabricated through direct metal laser sintering (DMLS). *J. Alloys Compd.* **2019**, *777*, 165–173. [CrossRef]
62. Zhou, M.; Lu, W.; Liu, X.; Zhai, W.; Zhang, P.; Zhang, G. Fretting wear properties of plasma-sprayed Ti3SiC2 coatings with oxidative crack-healing feature. *Tribol. Int.* **2018**, *118*, 196–207. [CrossRef]
63. Zhang, P.; Liu, X.; Lu, W.; Zhai, W.; Zhou, M.; Wang, J. Fretting wear behavior of CuNiAl against 42CrMo4 under different lubrication conditions. *Tribol. Int.* **2018**, *117*, 59–67. [CrossRef]
64. Zhai, W.; Lu, W.; Liu, X.; Zhou, L. Nanodiamond as an effective additive in oil to dramatically reduce friction and wear for fretting steel/copper interfaces. *Tribol. Int.* **2019**, *129*, 75–81. [CrossRef]
65. Zhai, W.; Zhou, K. Nanomaterials in superlubricity. *Adv. Funct. Mater.* **2019**, *29*, 1806395. [CrossRef]
66. Chen, X.; Zhai, W.; Dong, S.; Zheng, K.; Xu, R.; Wang, J.; Liu, X.; Lu, W. Investigations on torsional fretting wear properties of CuAlNi processed by ultrasonic vibration-assisted milling. *Tribol. Int.* **2020**. [CrossRef]
67. Kumar, S. Manufacturing of WC–Co moulds using SLS machine. *J. Mater. Process. Technol.* **2009**, *209*, 3840–3848. [CrossRef]

68. Kumar, S. Wear of SLS Materials under Plastic and Elastic Contact Conditions. 2008. Available online: http://edge.rit.edu/content/P10551/public/SFF/SFF%202008%20Proceedings/Manuscripts/2008-14-Kumar.pdf (accessed on 8 September 2019).
69. Naiju, C.; Anil, P.; Prashanth, M.M.; Karthik, S. Investigations on the lubricated wear of direct metal laser sintered components for functional applications. *ARPN J. Eng. Appl. Sci.* **2014**, *9*, 296–299.
70. Naiju, C.; Anil, P.; Mahadevan, A.; Kurian, J. Investigations on the Influence of Operating Parameters on the Lubricated Wear of SLS Materials. *Mater. Today Proc.* **2018**, *5*, 11319–11325. [CrossRef]